JOURNAL OF MATERIALS SCIENCE 32 (1997) 821–828

The effect of humidity on friction and wear of an aluminium–silicon eutectic alloy

BING K. YEN
Mitsubishi Kasei Research Centre, 1000, Kamoshida-cho, Midori-ku, Yokohama 227, Japan

The sliding wear of an aluminium–silicon eutectic alloy against cast iron counterface in 3–100% relative humidity range has been investigated. The results show that the moisture content has a significant effect on the friction and wear of the Al–Si alloy. The wear rate decreases by two orders of magnitude as the relative humidity increases from 3% to 100%. At low humidity conditions adhesive wear is predominant, whilst at high humidity conditions a layer of compacted oxide–metal debris film is formed on the Al–Si slider surface, which reduces the direct metal–metal contact. The friction coefficient is maximum at 3% and 100% relative humidity conditions.

1. Introduction

Due to their excellent castability, good strength to weight ratio and resistance to seizure under dry sliding conditions, aluminium–silicon alloys are widely used as bearing and piston materials in the automotive industry [1]. Experiments have shown that silicon in these alloys can decrease the propensity to seizure [2, 3] and most researchers agree that an optimal combination of mechanical properties and wear resistance can be obtained near the eutectic composition of 12.5 wt % [3–5]. However, the wear mechanisms of these materials are still far from clear.

Shivanath *et al.* [6] have shown that these materials undergo a transition from a mild wear regime to a severe wear regime at a given load when they slide against a steel counterface. The wear rates for the mild wear and severe wear regimes are in the range of 10^{-3}–10^{-2} $mm^3 m^{-1}$ and 1–10 $mm^3 m^{-1}$, respectively. Razavizadeh and Eyre [7, 8] have concluded that the mild wear regime is due to the oxidation wear of these alloys. Other researchers have also found a wear rate of the order of 10^{-3}–10^{-2} $mm^3 m^{-1}$ for loads up to 100 N but have attributed this mild wear regime to different mechanisms [9, 10]. Since Razavizadeh and Eyre [7, 8] have attributed the mild wear regime of aluminium–silicon alloys to the formation of oxides on the sliding surface, it is likely that the moisture content in the surrounding atmosphere may have an effect on the oxidation rate of the rubbing surfaces. This in turn would influence the friction and wear behaviour of these alloys. Moreover, Goto *et al.* [11] have found water vapour to influence the fretting wear of an aluminium alloy. Unfortunately, except in two studies [9, 10], most researchers have neglected to report the moisture content in the air at the time of their experiments.

The objective of the present investigation is to study the influence of moisture content on the unlubricated sliding wear of Al–Si alloys. Instead of superficially examining several Al–Si alloys, this study focuses only on the Al–Si eutectic alloy, which exhibits the highest wear resistance amongst, all Al–Si alloys. A commercial grade Al–Si eutectic alloy is rubbed against a cast iron counterface in air with a moisture content ranging from 3–100% relative humidity (RH). In addition to presenting the friction and wear results, the morphology and chemical composition of the Al–Si slider surface, counterface, and wear debris are examined systematically with scanning electron microscopy (SEM), energy dispersive X-ray spectroscopy (EDS) micro-analysis, and X-ray diffraction techniques.

2. Experimental procedure

JIS–AC8A, a commercial grade Al–Si eutectic alloy, was chosen for this study. The elemental composition of this alloy, shown in Table 1, is similar to that of LM13 and A336 alloys used in Europe and the United States, respectively [1]. Three sliders machined from the Al–Si alloy were evenly mounted onto the spindle of the testing machine at 120° spacing. The total apparent contact area was 75.4 mm^2. The counterface was machined from a grey cast-iron (JIS-FC250). The sliders and the counterface were first polished with #1500 grade and sand paper, and were then cleaned and degreased with acetone before mounting onto the apparatus.

A pin-on-disc type of apparatus was placed inside a 275 litre environmental chamber. The moisture content inside the chamber could be varied from 3–100% RH by flowing a mixture of dry air (60 ppm moisture content) and saturated air at 21 °C. The sliders rotated at a constant speed of 5 cm per s relative to the counterface. The experiment was conducted in a load range of 25–95 N, which is similar to that of other researchers [9, 10]. The sliding distance was 1 km for each set of experimental parameters.

0022–2461 © 1997 Chapman & Hall

TABLE I Chemical composition of JIS–AC8A base alloy*

Si wt%	Fe wt%	Cu wt%	Mg wt%	Ni wt%	Al wt%
12	0.8	1.1	1.0	1.2	Balance

* Ti, Mn, Zn, all less than 0.2 wt%

The friction force was recorded with an analog chart recorder and the wear rate was determined from weight loss measurements. Worn surfaces and debris were examined with a Hitachi S4100 scanning electron microscope equipped with EDS spectroscopy (Kevex Corporation) that is capable of detecting elements as light as boron under suitable conditions. The presence of oxides, if any, can be readily detected by the present equipment. Since many researchers [4, 5, 7, 8] have attributed the tribological characteristics of Al–Si alloys to a dark surface layer with thickness of 1–3 μm, the EDS micro-analysis was done at 20 kV to give an electron penetration depth of 1–2 μm. In addition to the elemental analysis by the EDS method, the chemical composition of the wear debris was analysed by X-ray diffraction method (Cu-K_α radiation).

3. Results

3.1. Influence of load at 50% RH

The Influence of load on friction and wear of the Al–Si eutectic alloy at 50% RH condition is first examined.

3.1.1. Friction and wear rates

Fig. 1 shows the wear of the Al–Si alloy as a function of the sliding distance under different loads. The volume loss increases linearly with the sliding distance in the load range of 25–95 N. Fig. 2 shows the wear rate and the friction coefficient of the Al–Si alloy at different loads. The friction coefficient remains relatively constant while the wear rate increases linearly with increasing load. In 50% RH air and a load range of 25–95 N the wear increases linearly with increasing sliding distance and load, which follows the adhesive wear law for metals proposed by Archard [12] and also Burwell and Strang [13]. No wear transition has been observed in the tested load range. The results from Pramila Bai and Biswas [9] are also shown in Fig. 2 for comparison. Both the wear rate and friction coefficient found in this study are slightly lower than that of Pramila Bai and Biswas, whose experiments were conducted using a hardend steel counterface in 40% RH air.

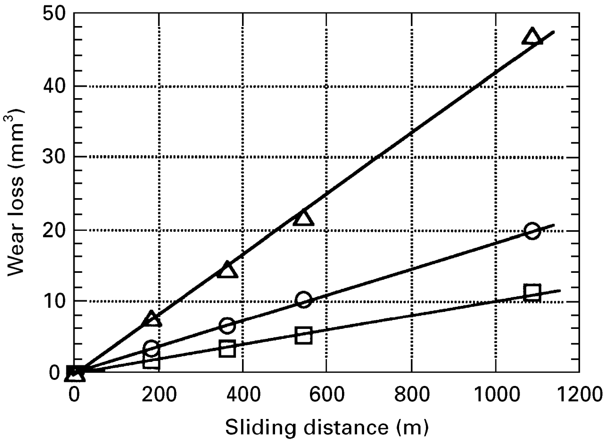

Figure 1 Wear of the Al–Si eutectic alloy versus sliding distance in 50% relative humidity air. The loads considered were; (□) 27N, (○) 49N and (△) 95N.

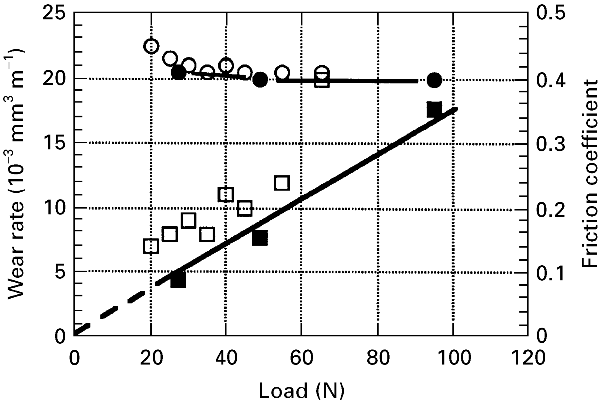

Figure 2 (■) Wear rate and (●) friction coefficient of the Al–Si eutectic alloy as a function of load in 50% relative humidity air. The wear rate (□) and friction coefficient (○) of Pramila Bai and Biswas [9] are also shown for comparison purposes.

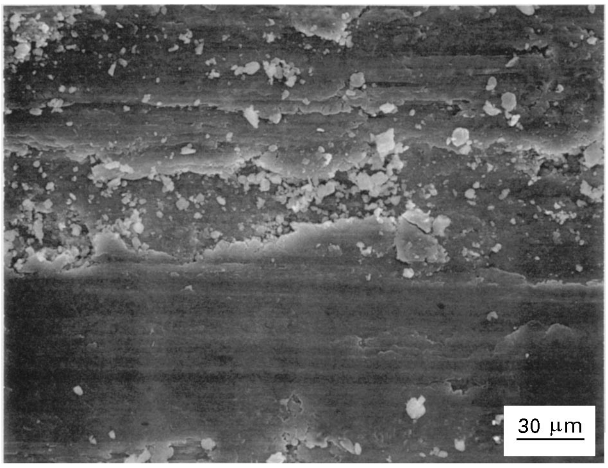

Figure 3 Worn Al–Si alloy slider surface showing scoring marks (95 N, 50% RH).

3.1.2. Surface morphology and chemical compositions

A worn Al–Si slider surface under a load of 95 N in 50% RH air is shown in Fig. 3. The sliding surface is relatively flat and marked with two types of wear scars. One type of scar is the scoring mark shown in the same figure. These scars are approximately 1–2 mm long and 10–30 μm wide and are oriented along the sliding direction. Other researchers [9, 10, 14] have also observed the same topography on Al–Si alloys of similar compositions. Due to the formation of a stratified layer structure on the sliding surface [4, 5], the valley region in the scoring scar is also relatively flat, resembling that of the unmarked region. A typical EDS spectrum of the flat contact surface is shown

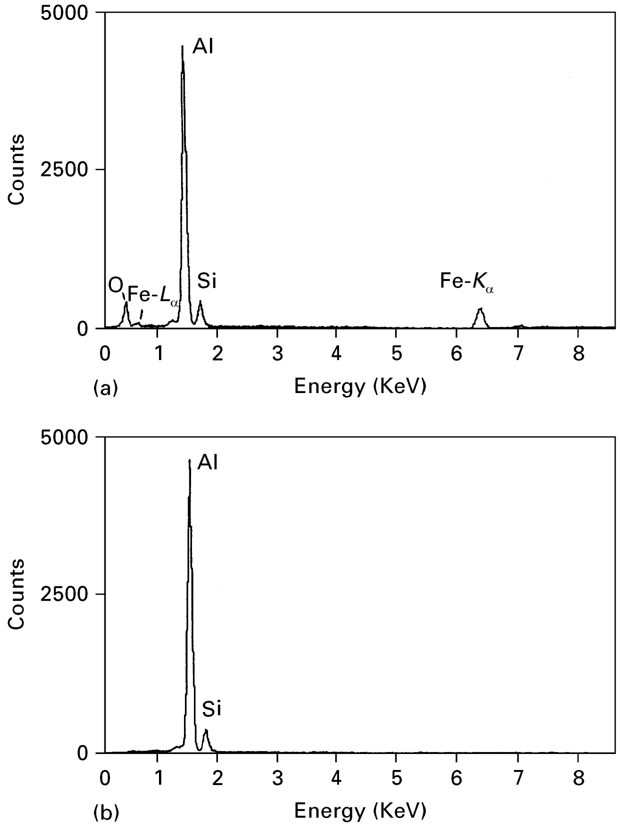

Figure 4 EDS spectra for (a) a worn Al–Si alloy slider surface (95 N, 50% RH) and (b) an unworn Al–Si alloy.

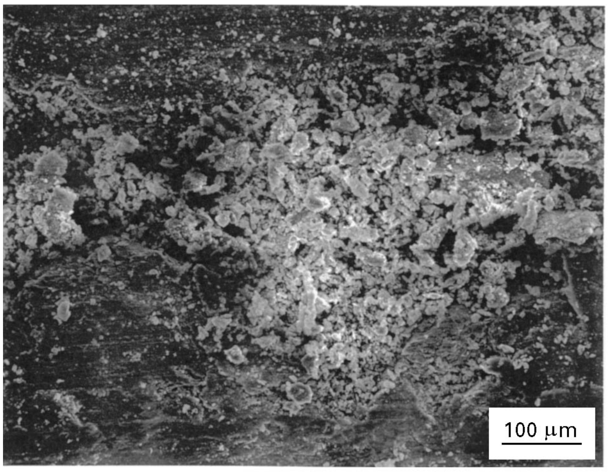

Figure 5 Worn Al–Si alloy slider surface showing craters filled with loose debris (95 N, 50% RH).

in Fig. 4a and for comparison and EDS spectrum of an unworn Al–Si alloy is shown in Fig. 4b. A small amount of iron from the counterface is detected on the worn surface, which agrees with the EDS results of other researchers [8, 10]. In addition to the Al, Si, and Fe peaks, a peak corresponding to oxygen can also be seen, which indicates the presence of oxide particles on the worn surface. Other researchers [8, 10], however, did not find a peak corresponding to oxygen. This is probably due to the limited sensitivity of their instrument. The EDS spectrum of the valley region in the scoring mark is identical to that of the sliding surface shown in Fig. 4, which suggests that the two surfaces have the same structure.

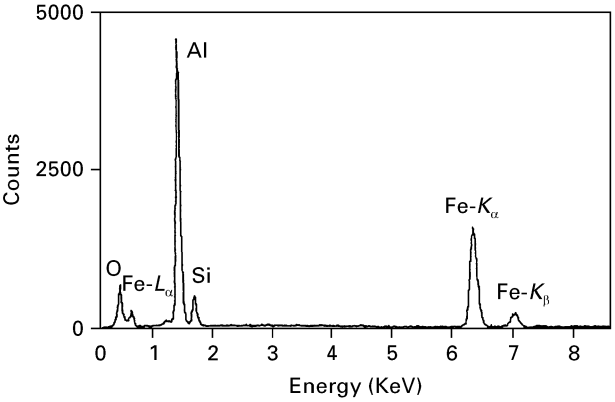

Figure 6 EDS spectrum of the debris found inside craters (95 N, 50% RH).

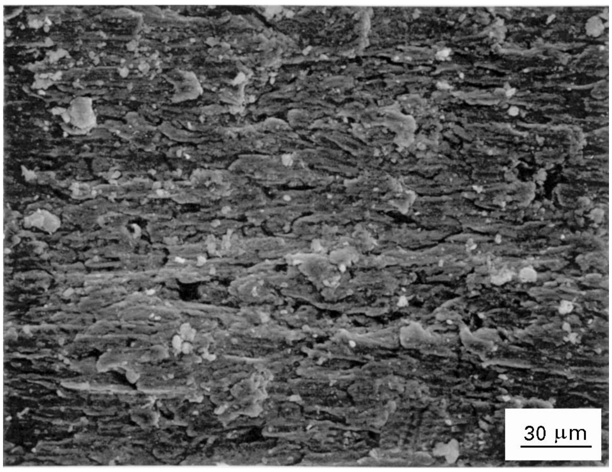

Figure 7 Worn cast iron counterface showing a scale-like surface morphology (95 N, 50% RH).

Galling marks shown in Fig. 5 are also found on the worn surface of the Al–Si alloy, especially near the leading edge of the slider. These craters are usually much larger and deeper than the scoring marks shown earlier. Moreover, craters on the sliding surface are usually filled with granular and plate-like debris particles. The EDS spectrum of the debris inside the crater shown in Fig. 6 indicates that a significant amount of iron particles from the counterface are present.

The worn counterface at 95 N load in 50% RH air is shown in Fig. 7. The scale-like surface morphology indicates that the cast iron sub-surface is grossly deformed by the friction force. The EDS spectrum of the iron counterface in Fig. 8 shows that Al and Si from the slider have transferred onto the surface. Approximately 10% of the worn counterface is covered with patches of aluminium transferred from the sliders as is shown in Fig. 9. Large scoring marks (~ 100 μm wide) filled with loose debris are also found on the surface. The loose debris has an identical elemental composition to that of the debris found on the slider surface shown in Fig. 6.

The worn surface of an Al–Si slider at a lower load (25 N) in 50% RH air is shown in Fig. 10. Although scoring scars are also present on the sliding surface, they are narrower and shorter as compared to those at a higher loading condition (Fig. 3). The sliding surface

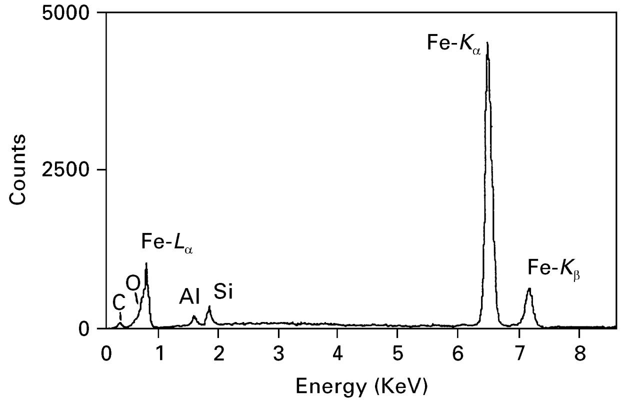

Figure 8 EDS spectrum of the worn cast iron counterface (95 N, 50% RH).

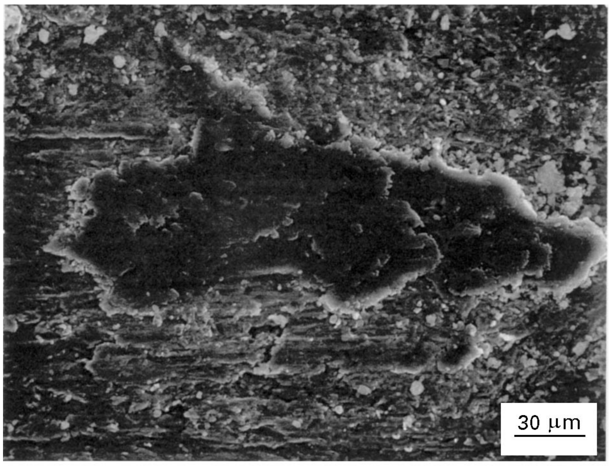

Figure 9 Patches of transferred aluminium on the cast iron counterface (95 N, 50% RH).

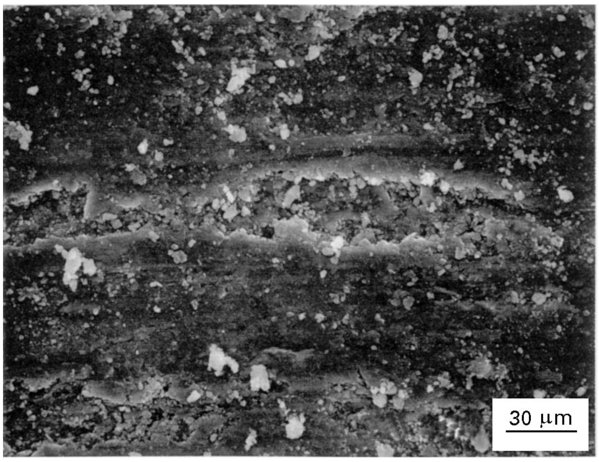

Figure 10 Worn Al–Si alloy slider surface at a lower load (25 N, 50% RH).

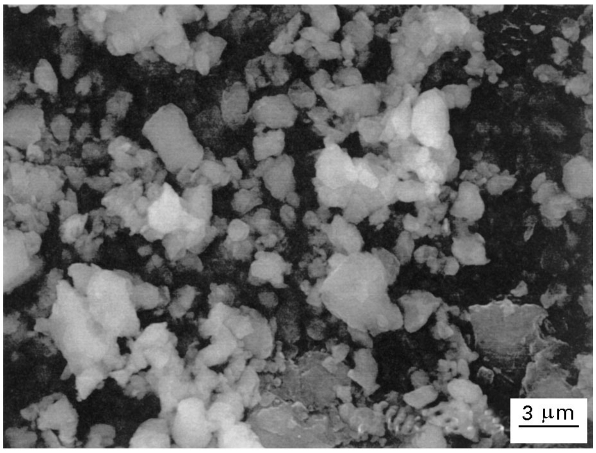

Figure 11 Granular debris particles found on the Al–Si alloy slider surface (25 N, 50% RH).

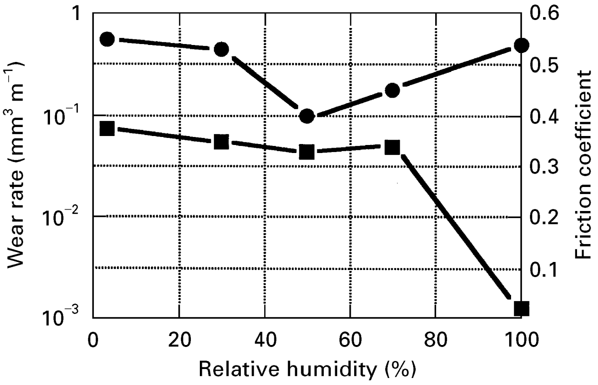

Figure 12 (■) Wear rates, and (●) friction coefficient of the Al–Si eutectic alloy at various humidity conditions (95 N).

appears to be composed of aggregates of granular particles. Furthermore, the valley region in the wear scar has a granular texture. Even though the surface morphology is slightly different from that observed at a higher load, the EDS micro-analysis shows that the sliding surface at a 25 N load has the same chemical composition (Fig. 4a). Besides scoring marks, craters filled with equiaxed debris particles also exist on the surface. However, they are smaller and fewer in number under the lighter loading condition. Fig. 11 shows the iron-rich debris found on the worn Al–Si surface. The debris particles consist mainly of equiaxed particles with a diameter of the order of 1 μm. The iron counterface at 25 N also has a scale-like surface morphology, which implies that the counterface material is removed mainly by an adhesive process. Although approximately 30% of the counterface surface is covered with a layer of loose debris particles, aluminium transferred patches like the one observed at higher load conditions (Fig. 9) are conspicuously absent.

3.2. Influence of moisture content

3.2.1. Friction and wear rates

Fig. 12 shows the wear rate and the friction coefficient of the Al–Si alloy as a function of relative humidity under a load of 95 N. The wear rate is highest at 3% RH (60 ppm of moisture). It decreases with increasing the relative humidity to 50% and then drops by two orders of magnitude at 100%, which suggests the existence of a wear transition point between 70–100% RH. The friction coefficient also decreases with increasing moisture content up to 50% RH. However, it then increases thereafter. Although the relationship between friction force and wear in sliding contact is still not clear, one would intuitively expect that an increase in friction force to concur with an increase in wear rate as observed in the 3–7% RH range. However, the wear rate drops by two orders of magnitude, while the friction coefficient increases to a maximum value of 0.54 at 100% RH, suggesting that a different wear mechanism is operating at the high humidity condition. Furthermore, the wear rate at 100% RH is at least one order of magnitude smaller than all previously reported values under a similar load condition [6, 9, 10].

3.2.2. Surface morphology and chemical composition

In addition to having a shiney metallic appearance, all worn Al–Si sliders under a load of 95 N in 3% RH air have a wedge formation at the leading edge [15, 16] and an approximately 1 mm long shear lip at the trailing edge, indicating severe plastic shear deformation below the surface. A shear lip at the trailing edge shown in Fig. 13 reveals that the surface is formed by layers of plastically deformed metal. A worn Al–Si slider surface under a load of 95 N in 3% RH air is shown in Fig. 14. The surface topography is similar to that of 50% RH shown in Fig. 3 except the scoring scars are usually wider (40–80 μm). Similarly in the 50% RH case, the valley region of the wear scar is relatively flat and has a similar texture to that of the surface. The EDS spectrum of the worn surface at 3% RH condition shown in Fig. 15 indicates that a small amount of iron has been picked up from the counterface. The chemical composition is similar to that observed in 50% RH (Fig. 4a) except that the oxygen count is almost zero. The wear debris inside the scar is composed of small equiaxed particles and large plate-like particles. The X-ray diffraction analysis of the debris sample shows that it is mainly composed of aluminium, silicon, and iron. The iron counterface at 3% RH has the same surface morphology and chemical composition as that of the counterface at 50% RH. However, aluminium transferred patches are rarely observed.

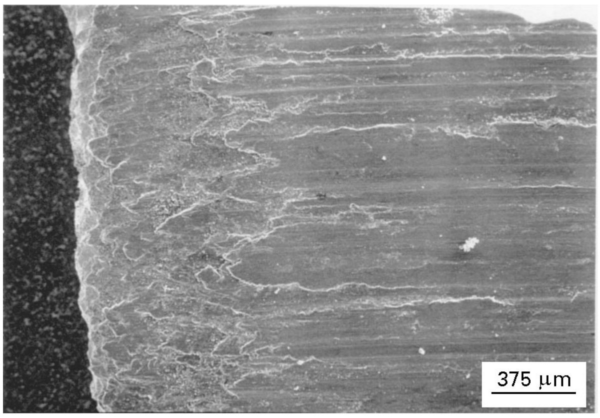

Figure 13 Worn surface at the trailing edge of an Al–Si alloy slider (95 N, 50% RH).

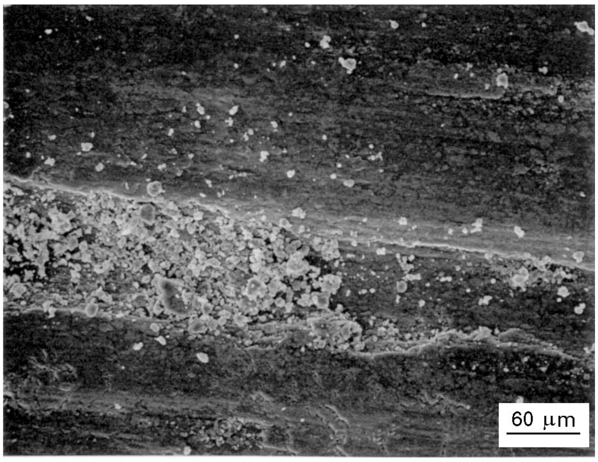

Figure 14 Worn Al–Si alloy slider surface in 3% relative humidity air (95 N).

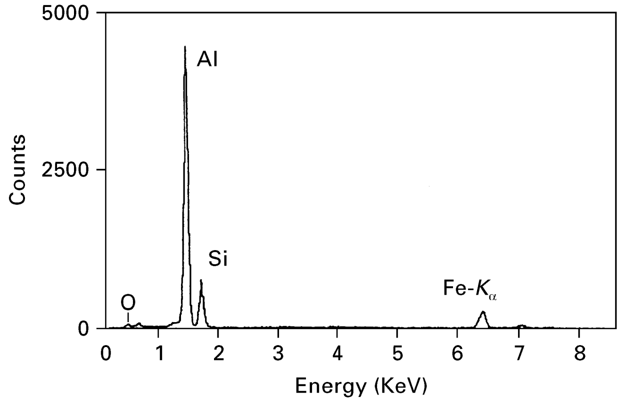

Figure 15 EDS spectrum of the worn Al–Si alloy surface in 3% relative humidity air (95 N).

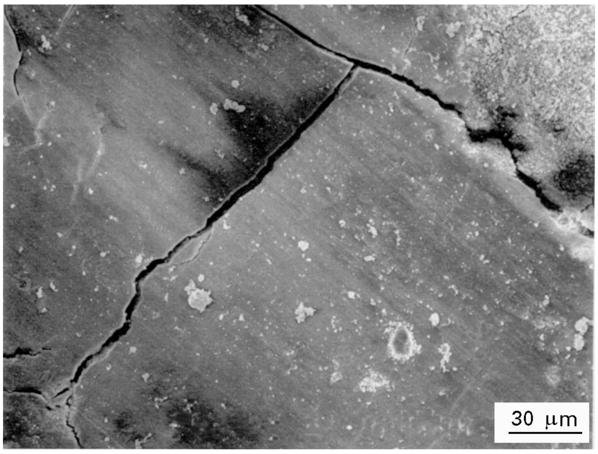

Figure 16 A debris film on the worn surface of the Al–Si alloy showing the formation craze cracks (95 N, 100% RH).

The general surface morphology and chemical compositions of the Al–Si sliders in the intermediate humidity range (30–70% RH) are similar. The flat sliding surface is marked with lines of scoring scars as previously shown in Fig. 3. The EDS analysis indicates that the surface contains a small amount of oxide. In the same humidity range the cast iron counterface has a scale-like surface morphology and part of the counterface is covered with patches of transferred aluminium.

All worn Al–Si slider in 100% RH air are completely covered with a black debris film. Unlike that at 3% RH condition, no wedge or shear lip is formed on the slider despite having a high friction coefficient. Fig. 16 shows a worn surface of an Al–Si slider at the

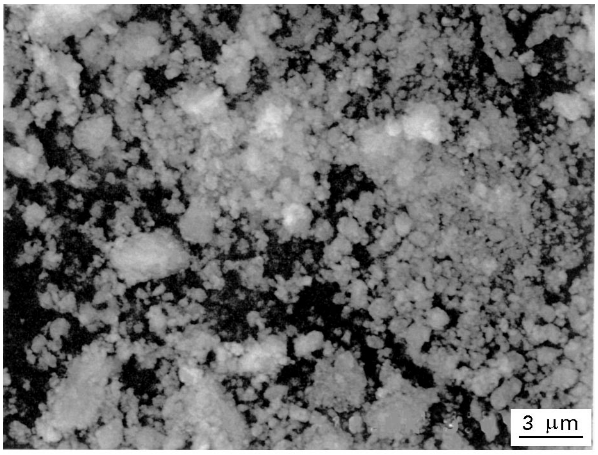

Figure 17 A magnified view of the debris film found on the Al–Si slider surface (95 N, 100%).

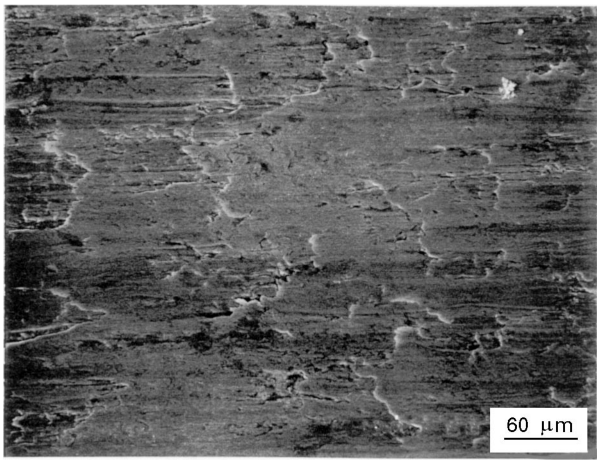

Figure 19 Worn cast iron counterface at 100% RH condition (95 N).

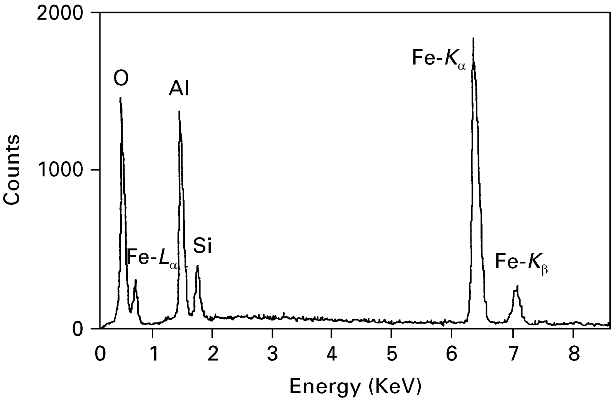

Figure 18 EDS spectrum of the debris film found on the Al–Si slider surface (95 N, 100%).

100% RH condition. The entire slider surface is covered with a thick smooth film that contains a network of craze cracks, which is very different from that observed at lower humidity conditions (3–70% RH). A magnified view of this surface in Fig. 17 shows that the film is made from the compaction of small equiaxed particles with diameters of 0.2–2 μm. The EDS spectrum of the same surface is shown in Fig. 18. The strong oxygen peak indicates that the debris film contains a large amount of oxide particles. It is tempting to suggest that this oxide film is formed by an oxidation–ploughing–compaction process of aluminium as proposed by Razavizadeh and Eyre [7, 8], but the X-ray diffraction analysis shows that Fe_2O_3 is the only oxide in the wear debris.

The iron counterface at 100% RH is shown in Fig. 19. The characteristic scale-like surface is severely flattend in this case. The flatness of the debris film on the sliders and counterface indicates a large true contact area, which explains the high friction coefficient observed. Although the Al–Si slider is covered with a continuous layer of debris film containing Fe_2O_3 particles, transferred material is rarely observed on the iron counterface. The EDS analysis of the iron counterface at the 100% RH condition is indistinguishable from that of lower humidity conditions despite the presence of large quantities of Fe_2O_3 in the debris and on the slider surface.

4. Discussion

4.1. Effect of moisture induced surface morphology on friction and wear

In the low and intermediate relative humidity range of 3–70%, the topography of the Al–Si slider is characterized by a smooth surface with a stratified layer structure. The surface is usually marked with long scoring marks and galling craters. In the same humidity range the iron counterface exhibits a scale-like surface topography. At the 3% RH condition, no transferred patch is observed either on the slider or on the counterface. Furthermore, the oxide content on the sliding surfaces is extremely low. The lack of transferred patches and oxide particles on the sliding surfaces increases the possibility of direct metal–metal contact, which causes the wear rate and friction coefficient to be high. The decrease in wear rate with increasing humidity shown in Fig. 12 is due to the increase of aluminium transferred patches on the counterface. These transferred patches reduce direct contact between the slider and the counterface and thus reduce the wear rate. Similarly, the decrease in the friction coefficient with increasing the relative humidity to 50% can also be explained by a decrease in the true contact area between the slider and counterface owing to the transferred patches. However, further increase in the humidity beyond 50% RH causes the true contact area to increase again due to an increase in the number of transferred patches, which leads to a higher friction coefficient.

At the 100% RH condition, the wear rate of the Al–Si alloy drops by two orders of magnitude whilst the friction coefficient reaches a maximum value of 0.54. The low wear rate is due to the continuous coverage of a debris film on the Al–Si surface as shown in Fig. 16, which reduces the direct contact between the sliders and counterface. The formation of a smooth counterface surface and a debris film indicates a large true contact area, which causes the friction coefficient to increase.

4.2. Wear mechanisms

The discussion of the wear mechanisms is divided into two wear regimes distinguished by the steep drop in the wear rate curve shown in Fig. 12. Since most investigators have neglected to report the humidity content in the air, it is reasonable to assume that their experiments were carried out in the 30–70% RH range to enable comparison of results.

4.2.1. *Low and intermediate humidity conditions (3–70% RH)*

The extensive formation of scoring marks and long shear lips and the lack of oxide particles on the surface clearly indicate that the "adhesive" type of wear is predominant at very low humidity conditions (3% RH). The adhesive wear is probably induced by the failure of graphite as a lubricant at low humidity conditions on the cast iron counterface [17, 18].

At the intermediate humidity range of 30–70% RH, the interpretation of a wear mechanism becomes less obvious due to the presence of a small amount of oxide on the Al–Si surface and the formation of aluminium transferred patches on the iron counterface. Moreover, the nature of the oxide cannot be determined from the EDS spectrum (Fig. 4a) alone since a small amount of iron is always present on the worn surface and both iron and aluminium can form stable oxides in air. In order to eliminate the uncertainty associated with the presence of iron, the experiment was repeated using an Al–Si counterface in 50% RH air. The resulting EDS spectrum of the worn slider shown in Fig. 20 is identical to that shown in Fig. 4a except for the lack of iron peaks, which suggests that the oxygen peak is attributed to an oxide of aluminium. Although Razavizadeh and Eyre [7, 8] have attributed the mild wear of Al–Si alloy to the formation of a compacted aluminium oxide debris film on the surface, the EDS spectrum (Fig. 4a) of the worn Al–Si surface shows that the oxide concentration is minimal. If the worn surface is covered with a layer of compacted oxide film, then the oxygen peak in the EDS spectrum should be much stronger similar to that shown in Fig. 18. Furthermore, other earlier investigations [9, 10] have found little or no aluminium oxide in the wear debris using X-ray diffraction techniques. It should be noted that Razavizadeh and Eyre [8] have detected aluminium oxide on the worn surface of Al–Si using X-ray photoelectron spectroscopy (XPS). However, one should be reminded that the effective depth of XPS analysis is approximately 5 nm and a piece of unworn aluminium in air will typically form an oxide layer of ~ 2 nm thickness. Therefore, the detection of aluminium oxide by the XPS method does not necessarily indicate that the 1–2 μm thick stratified surface layer is formed by the compaction of aluminium oxide. In light of the present results, it is unlikely that the worn Al–Si surface is formed by the compaction of oxide particles in the intermediate humidity range of 30–70% RH and a 25–95 N loading condition.

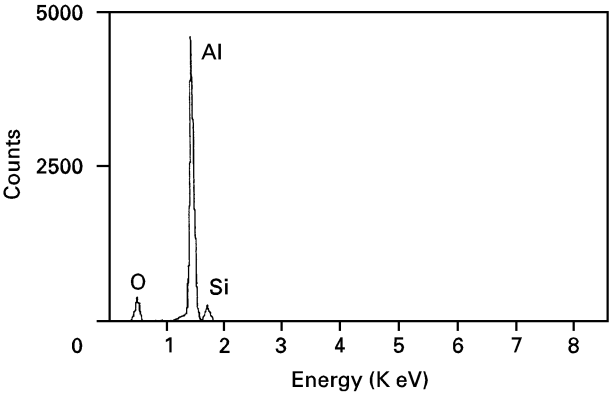

Figure 20 EDS spectrum of a worn Al–Si pin sliding against an Al–Si counterface (95 N, 50% RH).

While the worn surface of Al–Si is not formed from the compaction of oxide particles, it does contain a small amount of oxide. Since oxygen does not diffuse into the subsurface of the base alloy to form oxide particles, the worn surface layer is probably formed by the compaction of metallic debris particles that contain a thin oxidized layer on the particle surface. Such a structure can be formed by the redeposition and smearing of wear debris particles and/or a transfer and back-transfer mechanism [4, 10, 19] as suggested by the presence of aluminium transferred patches on the counterface.

4.2.2. *High humidity condition (100% RH)*

Although the oxidation wear mechanism through the formation of an aluminium oxide debris film as proposed by Razavizadeh and Eyre [7, 8] is questionable, the general concept is extremely suggestive; namely that oxide particles formed on a metal surface are removed and then compacted to form a debris film. Clearly, the formation of an oxide debris film through this mechanism depends on various factors that may influence the oxidation kinetics of the metallic system, such as temperature and moisture content. At high humidity conditions, an iron surface is readily oxidized to produce Fe_2O_3 particles [20], which are then removed from the surface as wear debris. The Fe_2O_3 debris particles and metallic debris particles are then compacted to form a smooth debris film on the Al–Si alloy surface. In addition to the thermodynamic factor, the formation of such a debris film would also depend on the generation of wear debris from the iron counterface. Therefore, eutectic and hypereutectic alloys with significant silicon content, which are known to wear even the hardest steel counterface [3], are more likely to form this type of surface compared to hypoeutectic alloys with low silicon content. Clark and Sarkar [4] have also observed a similar topography on a hypereutectic Al–Si alloy (21 wt % Si) at a much lower load and an unspecified humidity condition. The Auger spectrum of the same surface showed the presence of oxygen and iron on the surface.

Although the oxidative wear of aluminium may be possible at high temperature as the oxidation rate becomes significant, it is unlikely that the oxidation–ploughing–compaction process for aluminium as suggested by Razavizadeh and Eyre [7, 8] would occur at room temperature owing to the low oxidation kinetics.

5. Conclusions

Based upon the results obtained in this investigation, the following conclusions are drawn for the rubbing of an eutectic Al–Si alloy on cast iron in 3–100% RH range.

(1) The moisture content in the air can significantly influence the friction and wear behaviour of aluminium alloy–cast iron system.

(2) The wear rate of the Al–Si eutectic alloy in general decreases with increasing humidity.

(3) The wear mechanism of the Al–Si alloy changes from adhesive wear to a three-body type of wear as the relative humidity changes from 3 to 100%.

(4) Aluminium transferred patches and debris reduce the true contact between the slider and counterface, which results in a lower friction coefficient.

(5) Oxidation of aluminium is not a prevalent mechanism in the sliding wear in 3–100% RH range because of the low oxidation kinetics.

(6) The friction and wear behaviour of any metallic systems that contain ferritic materials would depend on the moisture content in the air, especially at high humidity conditions where the formation of Fe_2O_3 is thermodynamically favourable.

Acknowledgements

The author would like to thank Mr Asami of the Analysis Laboratory for the X-ray diffraction analysis of the debris samples.

References

1. B. S. SHABEL, D. A. GRANGER and W. G. TRUCKNER, in "Friction, Lubrication, and Wear Technology", edited by P. J. Blau (American Society for Metals, Metab Park, Ohio, 1992) p. 785.
2. P. K. ROHATGI and B. C. PAI, *Wear* **28** (1974) 353.
3. J. CLARKE and A. D. SARKAR, *ibid.* **54** (1979) 7.
4. *Idem.*, *ibid.* **82** (1982) 179.
5. K. MOHAMMED JASIM and E. S. DWARAKADASA, *ibid.* 119 (1987) 119.
6. R. SHIVANATH, P. K. SENGUPTA and T. S. EYRE, *Br. Foundryman* **70** (1977) 349.
7. K. RAZAVIZADEH and T. S. EYRE, *Wear* **79** (1982) 325.
8. *Idem.*, *ibid.* **87** (1983) 261.
9. B. N. PRAMILA BAI and S. K. BISWAS, *ASLE Transaction* **29** (1986) 116.
10. R. ANTONIOU and D. W. BORLAND, *Mater. Sci. Engng* **93** (1987) 57.
11. H. GOTO, M. ASHIDA and K. ENDO, *Wear* **116** (1987) 141.
12. J. F. ARCHARD, *J. Appl. Phys.* **24** (1953) 981.
13. J. T. BURWELL and C. D. STRANGE, *ibid.* **23** (1952) 18.
14. B. N. PRAMILA BAI, S. K. BISWAS and N. N. KUMTEKAR, *Wear* **87** (1983) 237.
15. M. COCKS, *J. Appl. Phys.* **33** (1962) 2152.
16. M. COCKS, *ibid.* **35** (1964) 1807.
17. D. H. BUCKLEY, NASA-TP-1052 Report, Effect of Carbon Content on Friction and Wear of Cast Irons (1977).
18. R. H. SAVAGE, *J. Appl. Phys.* **19** (1948) 1.
19. M. KERRIDGE and J. K. LANCASTER, *Proc. R. Soc. London* **A236** (1956) 250.
20. H. H. UHLIG and R. W. REVIE, in "Corrosion and Corrosion Control" (John Wiley & Sons, New York, 1985) p. 174.

Received 27 May 1994
and accepted 13 February 1996